Editors' Suggestion | Featured in Physics

Optofluidic Resonance of a Transparent Liquid Jet Excited by a Continuous Wave Laser

H. Liu,[1] Z. Wang,[1] L. Gao,[1,2] Y. Huang,[3] H. Tang,[2] X. Zhao,[1,*] and W. Deng[1,4,†]

[1]*Department of Mechanics and Aerospace Engineering, Southern University of Science and Technology (SUSTech), Shenzhen 518055, China*

[2]*Department of Mechanical Engineering, the Hong Kong Polytechnic University, Hong Kong, China*

[3]*State Key Laboratory of Digital Manufacturing Equipment and Technology, Huazhong University of Science and Technology, Wuhan 430074, China*

[4]*SUSTech Center for Complex Flows and Soft Matter Research, Shenzhen 518055, China*

(Received 26 June 2021; accepted 22 October 2021; published 10 December 2021)

We report a new optofluidic resonating phenomenon that naturally links the optical radiation pressure, total internal reflection, capillary wave, and Rayleigh-Plateau instability together. When a transparent liquid jet is radiated by a focused continuous wave laser beam, the highly ordered periodic jet breakup is unexpectedly triggered and maintained. The capillary wave enables the liquid-gas interface to serve as a rotating mirror reflecting the laser beam in a wide range of angles, including the critical angle for total internal reflection. The liquid jet acts as an optical waveguide to periodically transmit the laser beam to the upstream of the jet. The periodic optical beam transmittance inside the liquid jet exerts time-dependent optical pressure to the jet that triggers the Rayleigh-Plateau instability. The jet breakup process locks in at the frequency corresponding to the peak growth rate of the Rayleigh-Plateau instability of the liquid jet, which agrees with the prediction from the dispersion relation of a traveling liquid jet.

DOI: 10.1103/PhysRevLett.127.244502

Light carries a linear momentum and thus exerts a force upon reflection, refraction, or absorption on a surface [1,2]. The optical radiation force can be estimated by the ratio of power over speed of light. For 1-W optical power, the achievable optical force is in the nano-Newton range. Although this force appears to be weak by conventional standards, it may play dominant roles in many scientific and technological breakthroughs such as optical tweezers, radiation atom cooling, solar sail, optical juggling of droplets, among others [3–7]. Particularly at the interface of two transparent media, the optical and interfacial dynamic effects may couple and lead to new phenomena. For example, the radiation pressure is shown to bend liquid interfaces with high-power lasers, or with two liquids of very small interfacial tension, or through total internal reflections (TIR) [8–12]. On the other hand, a liquid jet is subject to the Rayleigh-Plateau instability [13] that exponentially amplifies perturbations of wavelength greater than the jet circumference. Therefore, the feeble optical force and pressure exerted on the upstream of the jet may be amplified to dictate the downstream jet breakup outcome. Here, we report an intriguing new phenomenon: when a transparent liquid jet is radiated by a focused continuous wave (CW) laser beam, the highly ordered periodic jet breakup is unexpectedly triggered and maintained. We show that this optofluidic resonating phenomenon is the result of collective effects of the optical radiation pressure, TIR, capillary wave, and Rayleigh-Plateau instability.

The experimental setup is schematically illustrated in Fig. 1(a). The microjet is generated by pumping liquid out of a stainless-steel nozzle. The jet velocity v_j is adjustable from 1.0 to 2.0 m/s. The jet radius R is varied in the range of 60 to 250 μm by changing the nozzle inner diameter. Four liquids of different surface tension γ were tested: deionized water ($\gamma = 72$ mN/m), mixture of 10% ethanol +90% deionized water (48 mN/m), ethanol (22 mN/m), and 3M® HFE7200 (13 mN/m). The liquid jet is approximately inviscid because the Ohnesorge number, which compares viscous and capillary forces, is small (<0.03) in this work. The jet Weber number (β^2) that assesses the ratio of the inertia to surface tension is $\beta^2 = \rho R v_j^2/\gamma$. A CW laser is focused by a microscope object lens, producing a beam cone angle of ~13°. The focused laser beam intercepts the jet at point C. The laser wavelength is 520, 532, or 638 nm. The laser power is adjustable from 0.3 to 3.3 W. The size of the focal point is ~20 μm, which is much smaller than the jet diameter. We define the jet breakup length L_B as the distance between the nozzle exit and the location of the breakup point (i.e., jet radius becomes zero). The distance between the nozzle tip and the laser intercepting point is L_C. The phenomena are recorded with a high-speed camera (IX Camera 220) coupled with a microscope of $0.7 - 5\times$ magnification, which provides a resolving power up to 1.6 μm per pixel.

Figures 1(b)–1(f) show the typical experimental phenomena (see Movie 1 in Supplemental Material [14]). Immediately after the laser is turned on, the jet breakup

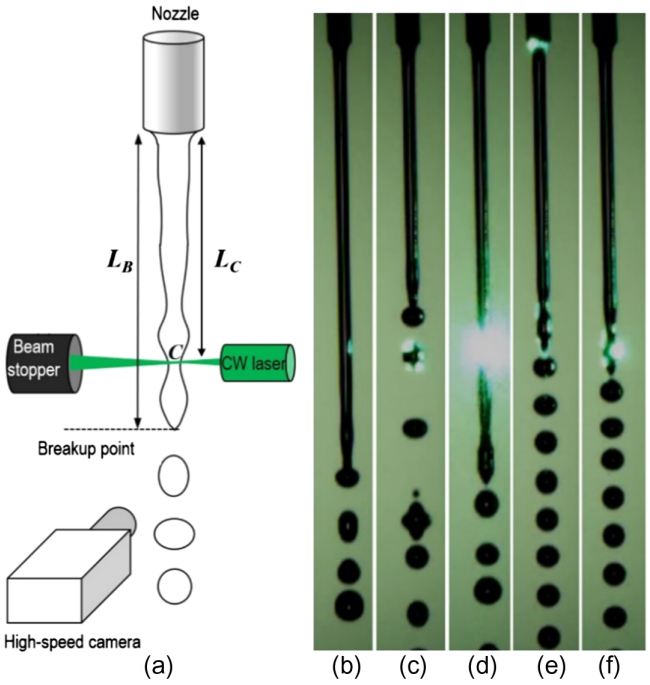

FIG. 1. (a) Schematic of the optofluidic resonance experiment. A focused CW laser beam intercepts the jet at point C. (b) Immediately after the laser is on, the jet breakup is still random. (c) The jet breakup point sometimes randomly moves up above C, showing the laser hits the droplet and generates multiple reflections inside the droplet. (d) Breakup point moves down and below C. (e),(f) ~100 ms after laser is on, the jet breaks up orderly. The exit of the nozzle is alternatively illuminated (e) or dark (f), indicating the laser beam is periodically transmitted upstream to the origin of the liquid jet. (Laser: 520 nm, 1.9 W; $R = 75$ μm; ethanol; flow rate: 1.4 mL/ min .)

remains random [Fig. 1(b)], and the breakup point hovers up [Fig. 1(c)] and down [Fig. 1(d)], with the breakup point randomly bracketing point C (the intersection point of the laser and jet). Particularly in Fig. 1(c), the jet breakup point is above C, showing that the laser beam hits the droplet and generates multiple reflections inside the droplet. This indicates that the laser focal point is indeed much smaller than the droplet diameter. About 100 ms after the laser is on, the breakup point position L_B stabilizes and eventually is pinned below the intercepting point [Fig. 1(e)]. The tip of the nozzle is alternatively bright [Fig. 1(e)] or dark [Fig. 1(f)], indicating the laser beam is intermittently transmitted upstream to the origin of the liquid jet.

We term this transition from random to highly ordered jet breakup as *optofluidic lock-in*. Once locked-in, the breakup event is so repeatable that we call it *in resonance*, which can be demonstrated in several visually evident ways. For example, when the frame rate of the high-speed camera is set the same as the jet breakup frequency ($f_0 = 2201$ fps), the video appears to be stationary (see movie in Supplemental Material [14]). If the frame rate is $f_0 - 1$, the breakup motion appears to be dramatically slowed

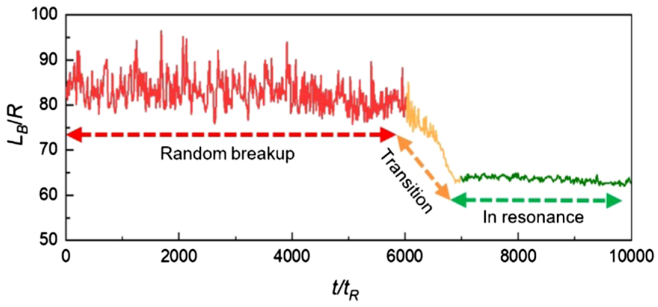

FIG. 2. Breakup point location history covering the entire process after laser is on, with the laser-jet intersecting point fixed (ethanol; $R = 109$ μm; $\beta^2 = 5$; laser: 532 nm, $P_L = 3.3$ W).

down [14]. Such video with the stroboscopic effect is only possible for highly repeatable periodic events. With the event frequency of f_0 and camera speed of f_0-1, the equivalent interval between two consecutive frames is f_0^{-1}-$(f_0\text{-}1)^{-1}$, yielding an apparent frame rate of $f_0(f_0\text{-}1) \sim f_0^2$, or 4.64×10^6 fps in our experiment.

The optofluidic lock-in is also accompanied by a significantly shortened jet length L_B, reduced swing of breakup point location, and narrowed droplet size distribution. For a typical case in Fig. 2, with laser-off, the dimensionless breakup length L_B/R is 84 ± 10 [Fig. 2(a)]. After the laser is switched on, L_B/R remains unchanged at first; 100 ms (or $\sim 10^3 t_R$) later, L_B/R gradually decreases to 64 ± 2, with both L_B and the fluctuation in L_B markedly reduced. Here, t_R is the capillary time $t_R = (\rho R^3/\gamma)^{1/2}$, where ρ is the liquid density. For random jet breakup, the relative standard deviation of the droplet diameter is ~20%. The polydispersity is partially attributed to the remerging of neighboring droplets (Supplemental Material, Fig. S1 [14]). Once the jet is in optofluidic resonance, the droplets are highly monodispersed without droplet merging due to identical droplet speed and constant interdroplet distance, consequently the relative standard deviation narrows down to ~1% (Supplemental Material, Fig. S1 [14]).

The optofluidic lock-in can be triggered by a range of laser power P_L and laser interception position L_C, regardless of laser wavelength. Fig. 3 shows the envelope of P_L and L_C obtained experimentally for ethanol jet ($R = 109$ μm). Three different breakup states I, II, and III are shown in Fig. 3(a). Region I represents the "optofluidic resonance" state. Regions II and III are collectively termed as "disordered" states because the jet does not break up evenly. In region II, the laser power is too weak to trigger resonance; while in region III the laser power is so high that the breakup point may move above the laser interception point to disrupt laser-jet coupling. Generally speaking, higher laser power leads to wider range of L_C. The shorter the L_C, the stronger the laser power is required to trigger jet resonance. We observe that as the laser interception point moves up, the breakup point tags along with it within a certain range.

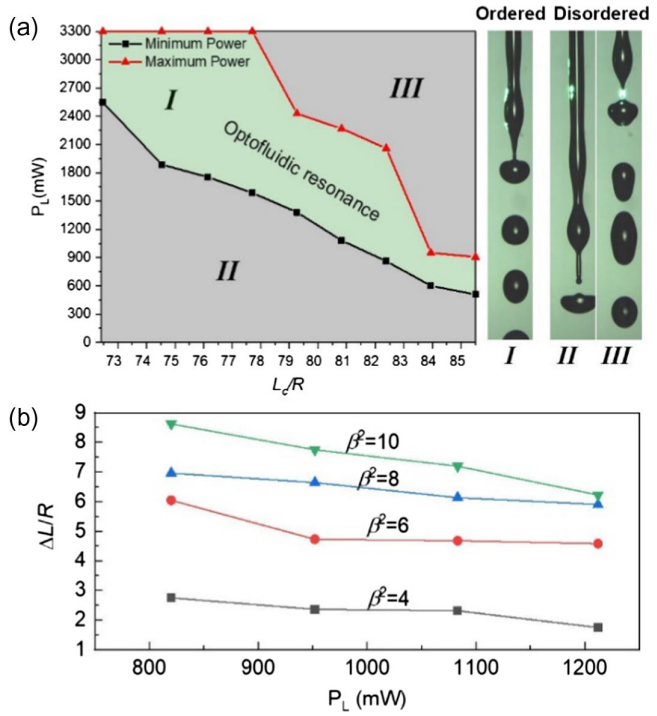

FIG. 3. (a) Envelope of the laser power (P_L) and the laser interception location (L_C) for triggering optofluidic resonances ($\beta^2 = 6$). (b) The difference between the interception location and breakup point at different laser power P_L and Weber number. (Ethanol; fixed $L_C/R = 83$; $R = 109$ μm; laser wavelength: 532 nm.)

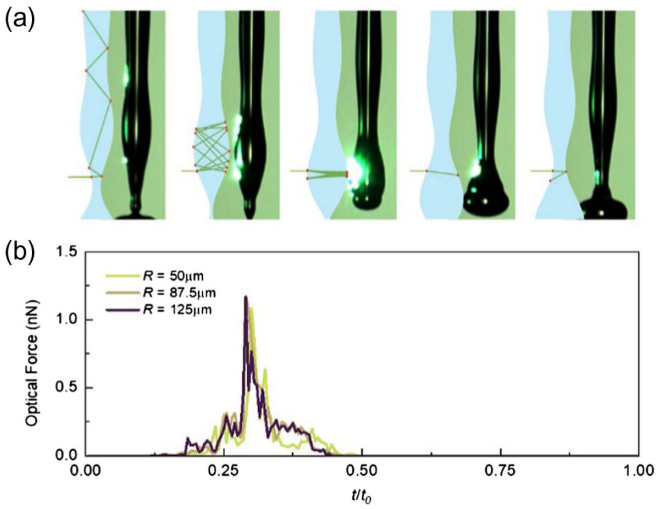

FIG. 4. Ray optics simulation. (a) Comparison of the simulation and experimental images at different stage of the traveling capillary wave (central axial plane) (ethanol; $R = 109$ μm; $\beta^2 = 6$; $P_L = 3.3$ W). (b) Optical force near the nozzle exit in a complete breakup period. "Near" is defined as within the distance of $2\pi R$ from the nozzle exit (ethanol; $\beta^2 = 6$; $P_L = 3.3$ W).

The difference of the interception position and breakup point ($\Delta L = L_B - L_C$) increases for greater jet Weber number, but ΔL decreases for higher laser power [Fig. 3(b)]. One way to understand the effect of Weber number (β^2) on ΔL is the following. The growth rate of perturbation is nearly a constant for different β^2; therefore, the time required for the same initial perturbation to grow into R is approximately the same. Within the same amount of time, the jet with larger β^2 travels further before breaking up. In addition, L_C is fixed in Fig. 3(a), hence $\Delta L/R$ increases with β^2.

The orderly breakup suggests that the jet is subject to a periodic perturbation of wave number k. The radial surface profile h of such a perturbed jet can be described by

$$h(z,t) = R - \varepsilon \exp(\omega_s z) \cos[k(z - v_j t)], \qquad (1)$$

where ε is the initial perturbation, ω_s is the spatial growth rate, and z is the jet axial direction. For the traveling jet with intermediate Weber numbers, spatial analysis is required [16]. We use the dispersion relation derived by Bogy [17] based on a one-dimensional Cosserat jet approximation [14] to determine f_B, which is the frequency corresponding to the fastest growth rate. The difference between the calculated f_B and measured resonance frequency f_0 is within 4% for $7.3 < \beta^2 < 15.4$ (Supplemental Material [14]). It supports the hypothesis that the resonance frequency converges to the frequency corresponding to the peak growth rate.

We found that less laser power is required to trigger the resonance for jets with lower surface tension for fixed jet radius. This is understandable because the lower the surface tension, the less the baseline Laplace pressure (γ/R) is, and less optical pressure will be required to cause the same amount of surface deformation. In addition, for lower surface tension, ΔL exhibits a wider range for the locked-in state, which suggests that the laser can affect the jet for a longer distance with liquids of lower surface tension. For example, for the liquid of very low surface tension (such as HFE7200), it will be much easier for the liquid jet to enter the optofluidic resonance state, where ΔL can be extended to up to $\sim 14R$ (Supplemental Material, Fig. S9 [14]).

To gain an understanding of the optical transmittance along the jet due to laser reflection and refraction, we conducted ray optics analysis [18,19] for the liquid jet with traveling capillary wave described by Eq. (1). For clarity, we only show the result of the center (or horizontal) beam, while the data of both 3D and axisymmetric jet profiles with focused Gaussian beams can be found in Supplemental Material [14]. Evidently, the jet surface near the breakup point serves as a rotating mirror that directs the laser beam upstream or downstream [Fig. 4(a)]. We refer the process of laser power trapped inside the jet through internal reflection as optofluidic coupling, and the ratio of trapped power P_t to injected power P_i as the coupling efficiency, i.e., $\eta = P_t/P_i$. After the laser beam enters the

jet, the incident angle of the first internal reflection is crucial because it determines the amount of laser power to be transmitted upstream. Moreover, the first reflection at the liquid-air interface determines the major loss of energy, because the subsequent reflection is more likely to be TIR. The maximum incident angle $\theta_{\max}$ upon the first reflection can be computed with the jet profile [Eq. (1)] near the breakup point, and $\theta_{\max} = \tan^{-1}(2\pi R/\lambda) + \theta_R \approx 46.7°$ for ethanol [14]. Here, θ_R is the refraction angle as the laser enters the liquid jet from the air side for the first time. $\theta_{\max}$ is close to the critical angle ($\theta_c = 47.3°$), and ~40% of the incident beam power will be reflected back inside the jet for ethanol. For the focused conical beam, it is reasonable to expect a significant portion of the beam will exceed θ_c and undergo TIRs. The complete ray tracing model suggests that the peak light coupling efficiency is 20%–40%, and the exact η depends on jet diameter as well as ΔL [14]. The analysis suggests that the coupling of the laser beam and the jet with capillary wave could be quite effective. Experimentally, we quantify η using a setup similar to the integrating sphere [14]. The measured $\eta(t)$ is consistent with that obtained from ray tracing model. For example, for the 109 μm radius ethanol jet, the measured peak η is about 40%, in good agreement with the calculated value.

In a single breakup period t_0, we obtain the optical forces numerically at each ray-interface interaction position by evaluating the momentum change of the incoming versus outgoing rays [Fig. 4(b)]. We varied the jet radius R while keeping the Weber number constant ($\beta^2 = 6$). The computed results suggest all jets experience comparable peak force of ~1.2 nN, and the optical force history in each breakup period appears to be self-similar for different jet radius [Fig. 4(b)].

As the capillary wave develops, the amount of laser power injected to the jet fluctuates periodically. Therefore, the entire jet is subject to the perturbation caused by the pulsating optical force and pressure. However, the optofluidic perturbation is most consequential and effective in the vicinity of the nozzle where the jet is formed because of two reasons. First, the initial perturbation requires time to grow into ~R to break up the jet. Therefore, the earlier the perturbation (or closer to the nozzle), more time will be allowed for the perturbation to develop. In other words, although the entire jet is subject to the pulsed optical force, the earlier perturbation has longer time to be amplified and eventually dictates the jet breakup. Second, the meniscus provides additional light trapping to concentrate the optical impulse near the nozzle. The ray tracing model shows that the meniscus near nozzle can enhance the optical impulse by about 34% [14].

To further confirm that the ordered breakup is due to the perturbation originated near the nozzle exit, we observed the jet behavior after the laser is turned off (Fig. 5). The jet breakup remains highly ordered and the produced droplets are monodispersed for a duration of ~6 ms (or ~$28t_R$) before the jet resumes to break up randomly. On the other hand, the distance between the breakup point to the nozzle exit is $L_B = 8.6$ mm, and the perturbation should travel at the same velocity of the jet $v_j = 1.45$ m/s. Therefore, the calculated time delay is $L/v_j = 5.9$ ms, in close agreement with the experiment (~6 ms). This data supports the hypothesis that the most effective perturbation is at the origin of the jet.

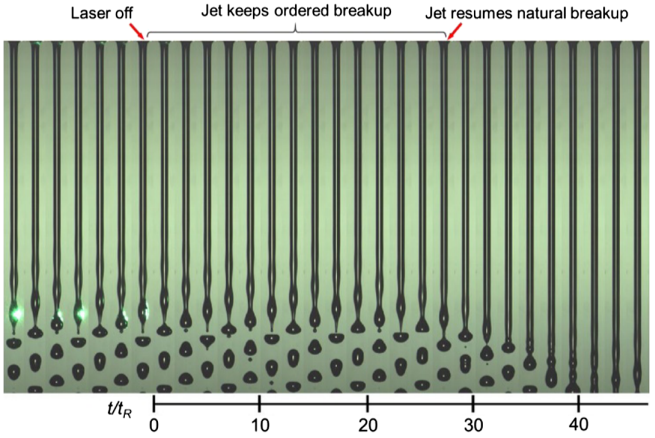

FIG. 5. The initially in-resonance ethanol jet keeps ordered breakup for ~$28t_R$ (or ~6 ms) after the CW laser is turned off ($R = 109$ μm; $v_j = 1.45$ m/s; $P_L = 3.3$ W).

The magnitude of the initial perturbation ε is typically too small to be measured directly from the image, especially for transient processes. Alternatively, ε can be inferred from L_B through the following analysis. We assume the perturbation grows to R at the breakup point, therefore

$$\varepsilon/R = \exp(\omega_s L_B). \tag{2}$$

The spatial growth rate ω_s is given by the imaginary part of the wave number from the dispersion relation [14,17]. For example, using the data of Fig. 2(a), ($v_j = 1.22$ m/s, $R = 109\,\mu$m, $L_B = 6.89$ mm), we obtain $\omega_s = -1444$ m^{-1}. Therefore, for unperturbed jets, the initial perturbation is estimated to be ~0.1 nm; while for perturbed jets, the corresponding ε is ~5 nm. Therefore, the periodic optical perturbation dominates over natural perturbations and dictates the breakup behavior.

Next, we argue that the thermal Marangoni effect [20] is negligible and is not responsible for the ordered jet breakup in this work. With the typical case of flow rate of $Q = 2.8$ mL/ min, $R = 109$ μm, $\beta^2 = 6$, $P_L = 2$ W, the change of radius due to thermal effect is estimated to be only ~1 pm [14]. This is indeed negligibly small compared with natural perturbation of ~0.1 nm. We also dyed the liquid with Acid Scarlet G (paired with 532 nm laser). Although the optical absorption is greatly enhanced, the resonance disappears. This is another evidence that the optofluidic resonance phenomenon is not thermally driven.

We now examine the possibility that the optical radiation pressure could be responsible for the initial deformation of a few nanometers. The optical force is $\sim P_t/c$. The optical power trapped by the jet is up to ~0.6 W for the 1.5 W incoming laser with a 40% peak coupling efficiency, therefore the maximum optical force due to reflection is ~2 nN. Assuming the liquid meniscus confines the light near the nozzle exit in an area of $\sim R^2$, we estimate the optical pressure is on the order of ~0.2 Pa. Such a change in Laplace pressure introduces the deformation in initial jet radius, and ε is estimated to be ~10 nm. This value is far greater than both the thermal effect and natural perturbations, while ε is also in line with the perturbation magnitude estimated from the breakup length. We note that [12] reported a surface bending caused by the TIR of a CW laser at the flat liquid-air interface. Although in [12] the phenomena are observed at steady state, the deformed surface in [12] exhibits a bending magnitude of ~10 nm at 600 mW for water—both the length scale and the effective laser power are comparable with the data reported in this work. We also compare ε in our work with the interface deformation by a high-power pulse laser in literature [10]. The 4 kW, 60 ns pulse laser in [10] produces a surface displacement of hundreds of nanometers [10], which is one order of magnitude greater than $\varepsilon \sim 10$ nm in our work. This is not surprising because the impulse of the high-power laser in [10] is approximately 10 times of the impulse for each breakup period in this work.

In summary, we found that the traveling capillary wave enables the liquid-air interface to serve as a rotating mirror that reflects the laser beam in a wide range of angles, including the critical angle for TIR. Under periodic TIRs, the liquid jet acts as an optical waveguide to transmit the laser beam and momentum to the upstream of the jet. The reflection inside the liquid jet is therefore periodic and exert time-dependent optical force that triggers the Rayleigh-Plateau instability. Such resonance quickly locks-in at the frequency associated with the peak growth rate of the liquid jet predicted by the dispersion relation of an inviscid liquid jet. We note that the Rayleigh-Plateau instability can be triggered by a few different ways, including mechanical vibration inside the nozzle [21] and an ac electric field around the liquid jet [22,23]. Our work provides evidence of the first optically triggered Rayleigh-Plateau instability by a CW laser. The phenomena reported here are truly optofluidic in nature because the optical power feeds the momentum through the liquid optical waveguide and critically affects the fluid dynamic outcome of the liquid jet. The CW laser illuminated jet also exhibits an automatic feedback and lock-in feature in a very simple form. It is almost like the jet can response, learn, and adapt to the external stimulation. The fact that the combination of two separately well-studied subjects (a simple liquid jet and a CW laser) can lead to unexpected phenomena is intriguing.

W. D. thanks the National Natural Science Foundation of China (No. 11932009, No. 11872199), Guangdong Provincial Innovation and Entrepreneurship Project (2017ZT07C071), and Guangdong Provincial Key Laboratory Program (2021B1212040001) for financial support.

*Corresponding author.
zhaoxy@sustech.edu.cn
†Corresponding author.
dengww@sustech.edu.cn

[1] H. M. Lai and K. Young, Phys. Rev. A **14**, 2329 (1976).
[2] I. I. Komissarova, G. V. Ostrovskaya, and E. N. Shedova, Opt. Commun. **66**, 15 (1988).
[3] A. Ashkin, Phys. Rev. Lett. **24**, 156 (1970).
[4] A. Ashkin, Phys. Rev. Lett. **40**, 729 (1978).
[5] A. J. Bae, D. Hanstorp, and K. Chang, Phys. Rev. Lett. **122**, 043902 (2019).
[6] W. D. Phillips, Rev. Mod. Phys. **70**, 721 (1998).
[7] A. Ashkin, Science **210**, 1081 (1980).
[8] N. Bertin, H. Chraibi, R. Wunenburger, J. P. Delville, and E. Brasselet, Phys. Rev. Lett. **109**, 244304 (2012).
[9] E. Brasselet, R. Wunenburger, and J. P. Delville, Phys. Rev. Lett. **101**, 014501 (2008).
[10] A. Ashkin and J. M. Dziedzic, Phys. Rev. Lett. **30**, 139 (1973).
[11] A. Casner and J. P. Delville, Phys. Rev. Lett. **90**, 144503 (2003).
[12] G. Verma and K. P. Singh, Phys. Rev. Lett. **115**, 143902 (2015).
[13] J. Eggers and E. Villermaux, Rep. Prog. Phys. **71**, 036601 (2008).
[14] See Supplemental Material at http://link.aps.org/supplemental/10.1103/PhysRevLett.127.244502 for the movie of jet resonance upon laser illumination, the process of restoring the random breakup after the laser is turned off, as well as more details, which includes Ref. [15].
[15] R. Wunenburger, A. Casner, and J. P. Delville, Phys. Rev. E **73**, 036314 (2006).
[16] J. B. Keller, S. I. Rubinow, and Y. O. Tu, Phys. Fluids **16**, 2052 (1973).
[17] D. B. Bogy, Phys. Fluids **21**, 190 (1978).
[18] A. Ashkin, Biophys. J. **61**, 569 (1992).
[19] E. Brasselet and J. P. Delville, Phys. Rev. A **78**, 013835 (2008).
[20] M. R. de Saint Vincent, H. Chraïbi, and J. P. Delville, Phys. Rev. Applied **4**, 044005 (2015).
[21] H. Duan, F. J. Romay, C. Li, A. Naqwi, W. Deng, and B. Y. Liu, Aerosols Sci. Technol. **50**, 17 (2016).
[22] H. González and F. J. García, J. Fluid Mech. **619**, 179 (2009).
[23] W. Yang, H. Duan, C. Li, and W. Deng, Phys. Rev. Lett. **112**, 054501 (2014).